Automated detection of diabetic retinopathy using SVM

Conference Paper · August 2017

DOI: 10.1109/INTERCON.2017.8079692

3 authors:

Enrique V. Carrera
Universidad de las Fuerzas Armadas-ESPE
107 PUBLICATIONS **2,074** CITATIONS
SEE PROFILE

Andrés González
Universidad de las Fuerzas Armadas-ESPE
1 PUBLICATION **38** CITATIONS
SEE PROFILE

Ricardo Carrera
Universidad San Francisco de Quito (USFQ)
4 PUBLICATIONS **39** CITATIONS
SEE PROFILE

Automated detection of diabetic retinopathy using SVM

Enrique V. Carrera
Dept. de Eléctrica y Electrónica
Univ. de las Fuerzas Armadas ESPE
Sangolquí, Ecuador
evcarrera@espe.edu.ec

Andrés González
Dept. de Eléctrica y Electrónica
Univ. de las Fuerzas Armadas ESPE
Sangolquí, Ecuador
spedygon007@gmail.com

Ricardo Carrera
Colegio Politécnico
Univ. San Francisco de Quito
Cumbayá, Ecuador
rvcarrera@estud.usfq.edu.ec

***Abstract*—Diabetic retinopathy is a common eye disease in diabetic patients and is the main cause of blindness in the population. Early detection of diabetic retinopathy protects patients from losing their vision. Thus, this paper proposes a computer-assisted diagnosis based on the digital processing of retinal images in order to help people detecting diabetic retinopathy in advance. The main goal is to automatically classify the grade of non-proliferative diabetic retinopathy at any retinal image. For that, an initial image processing stage isolates blood vessels, microaneurysms and hard exudates in order to extract features that can be used by a support vector machine to figure out the retinopathy grade of each retinal image. This proposal has been tested on a database of 400 retinal images labeled according to a 4-grade scale of non-proliferative diabetic retinopathy. As a result, we obtained a maximum sensitivity of 95% and a predictive capacity of 94%. Robustness with respect to changes in the parameters of the algorithm has also been evaluated.**

***Index Terms*—Diabetic retinopathy, digital image processing, machine learning, support vector machines.**

I. Introduction

Diabetic retinopathy is a severe and widely spread eye disease. It is the commonest cause of legal blindness in the working-age population of developed countries [1]. Diabetic retinopathy occurs when diabetes damages the blood vessels inside the retina, leaking blood and fluids into the surrounding tissue. This fluid leakage produces microaneurysms, hemorrhages, hard exudates, and cotton wool spots (*a.k.a.*, soft exudates) [2], [3]. Diabetic retinopathy is a silent disease and may only be recognized by patients when changes in the retina have progressed to a level where treatment becomes difficult or even impossible.

The increasing number of diabetic retinopathy cases worldwide requires to intensify efforts in developing tools to assist in the diagnosis of diabetic retinopathy. Automatic detection of diabetic retinopathy will lead to a large amount of savings of time and effort. Thus, Wu *et al.* [1] proposed a method for automatic detection of microaneurysms in retinal fundus images. In [4], Maher *et al.* already evaluated a decision support system for automatic screening of non-proliferative diabetic retinopathy. In fact, support vector machines were used by Maher *et al.* [5] in the automated diagnosis of non-proliferative diabetic retinopathy. Several image pre-processing techniques have also been proposed in order to detect diabetic retinopathy [6]–[9]. However, despite all these previous works, automated detection of diabetic retinopathy still remains a field for improvement [2].

Thus, this paper proposes a new computer assisted diagnosis based on the digital processing of retinal images in order to help people detecting diabetic retinopathy in advance. The main goal is to automatically classify the non-proliferative diabetic retinopathy grade of any retinal image. For that, an initial image processing stage isolates blood vessels, microaneurysms and hard exudates in order to extract features that can be used by a support vector machine (SVM) to figure out the retinopathy grade of each retinal image. The image database used in this study is the Messidor database [10]. A decision tree classifier is also implemented to contrast the results obtained with our SVM classifier.

Our proposal has been tested on a database of 400 retinal images labeled according to a 4-grade scale of non-proliferative diabetic retinopathy. As a result, we obtained a maximum sensitivity of 94.6% and a predictive capacity value of 93.8%. Robustness with respect to changes in the parameters of the algorithm has also been evaluated.

II. Methodology

There are two types of diabetic retinopathy: non-proliferative diabetic retinopathy (NPDR) and proliferative diabetic retinopathy, where the NPDR can be subdivided into mild, moderate and severe [3]. In fact, NPDR is the most common diabetic retinopathy, representing 80% of all cases.

The retinopathy grade diagnoses is normally provided by medical experts based on:

0. Normal (μA=0) and (H=0)
1. Mild NPDR ($0<\mu A\leq 5$) and (H=0)
2. Moderate NPDR ($5<\mu A<15$ or $0<H<5$) and (NV=0)
3. Severe NPDR ($\mu A\geq 15$) or ($H\geq 5$) or (NV=1)

where μA is the number of microaneurysms, H the number of hemorrhages and NV the presence of neovascularization.

A. Image database

The Messidor database [10] consists of 1200 eye fundus color numerical images of the posterior pole acquired by 3 ophthalmologic departments using a color video 3CCD camera on a Topcon TRC NW6 non-mydriatic retinograph with a 45 degree field of view. The images were captured using 8 bits per

978-1-5090-6363-5/17/$31.00

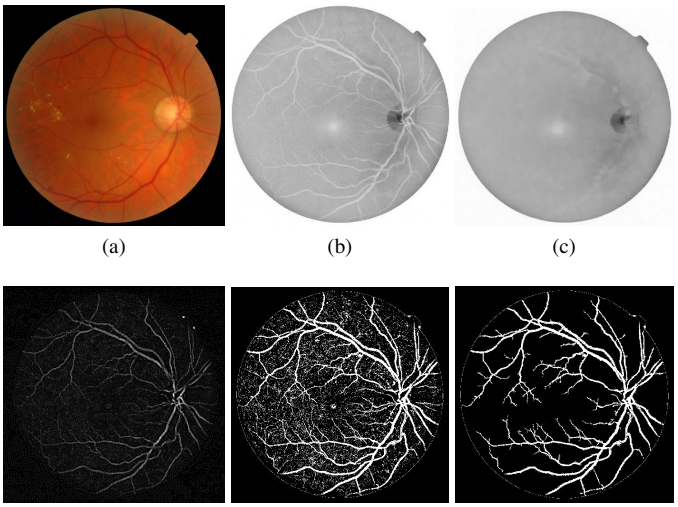

Fig. 1. Blood vessel detection: (a) Original image, (b) Magenta component, (c) Morphological processed image, (d) Difference between *b* and *c* images, (e) Binarized image, (f) Noise-reduced image.

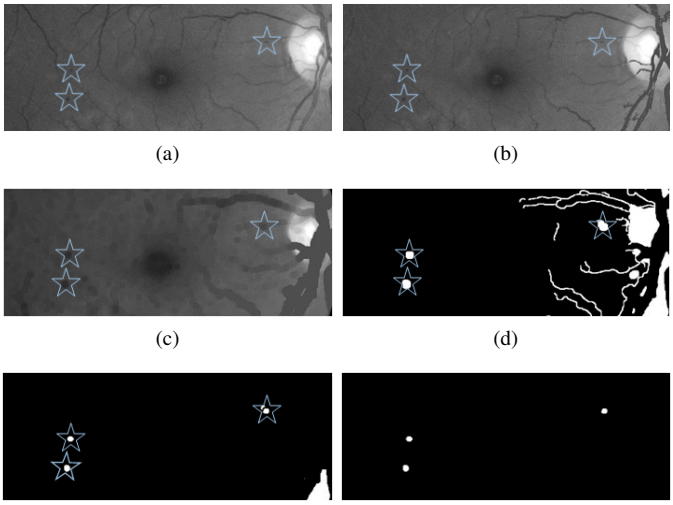

Fig. 2. Detection of microaneurysms (μA)—blue stars highlight final positions: (a) Green component, (b) Blood-vessel concealment, (c) Dilated image, (d) Edge detection and hole filling, e) Pre-selected μA, (f) Selected μA.

color plane at 1440×960, 2240×1488 or 2304×1536 pixels. 800 images were acquired with pupil dilation (one drop of Tropicamide at 0.5%) and 400 without dilation.

The 1200 images are packaged in 3 sets, one per ophthalmologic department, using the TIFF format. In addition, an Excel file with medical diagnoses for each image is provided. In this work, we use the images of just one ophthalmologic department containing 152 images without retinopathy (grade 0), 30 with mild NPDR (grade 1), 69 with moderate NPDR (grade 2), and 149 with severe NPDR (grade 3).

B. Extracted features

In order to automatically detect NPDR we have implemented three main processes to extract some important features. Additionally, the retina edge was previously segmented from the rest of the image using the red component of each retinal image.

1) Blood vessels: The aim of this initial process is to determine the blood-vessel density in a retinal image. For that, the RGB image is transformed to its CMY representation and the magenta component is isolated. On the magenta component, morphological operations (*i.e.*, erosion, opening, and dilation) hide blood vessels. The difference between the magenta component and the resulting image of the morphological processing is binarized after a histogram matching that increases its contrast. The noise existing in the binarized image is reduced through dilation and erosion operations. At the end, the density of white pixels (*i.e.*, blood vessels) in the last image is computed. Fig. 1 shows the resulting images at each stage of this process.

2) Microaneurysms: Microaneurysms are small lumps in the blood vessels, appearing as small and round shape dots near to tiny blood vessels. In order to determine the number of microaneurysms, the green component is extracted and the blood vessels are hidden using the noise-reduced image of the previous process. Basically, the pixels corresponding to blood vessels are painted with the average retina color. Next, a disc-based dilation operation is applied to highlight the microaneurysms. This image is then treated by edge-detection and hole filling algorithms to knit together the possible microaneurysms. It is important to find the difference between the resulting image and the image of edges to finally remove those edges. At the end, the possible microaneurysms are filtered by form and size using morphological operations and a maximum number of pixels to get the actual microaneurysms. The resulting images of this process are shown in Fig. 2.

3) Hard exudates: Detection of exudates is an important characteristic for diagnosis, and the clear color of them helps us to recognize them. In order to detect hard exudates, the magenta component is extracted from the CMY image and a threshold-based binarization depending on the standard deviation of the magenta component is applied. The binarized image is improved changing the retina contour to white color and adding the optical-disc mask. How to extract the optical-disc mask is explained in the next paragraph. Then, a dilation operation is applied to the resulting image and large continuous regions are removed. Finally, a erosion operation is executed before computing the density of hard exudates. The whole process is graphically summarized in Fig. 3.

The optical-disc mask mentioned in the previous paragraph is extracted using the green and cyan components. A graphical synopsis of the procedure is presented in Fig. 4. Both components are pre-processed by a histogram matching in order to highlight the optical disc. After that, the image resulting from the difference of both components is binarized and a disc-based dilation operation is applied. Using the Hough transform, the geometry of the optical disc is recovered and an optic-disc mask is created to match that geometry.

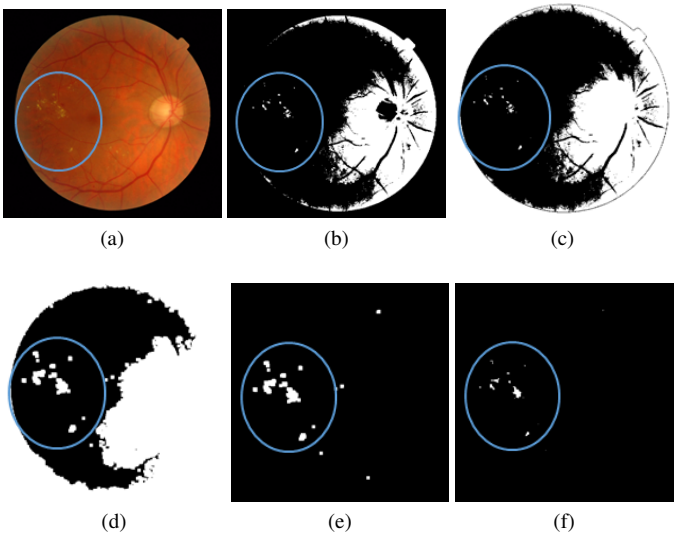

Fig. 3. Detection of hard exudates (*hE*)—a blue oval highlights region of interest: (a) Original image, (b) Color segmentation, (c) Background removal and optical-disc mask is added, (d) Dilated image, (e) Pre-selected *hE* (f) Finally selected *hE*.

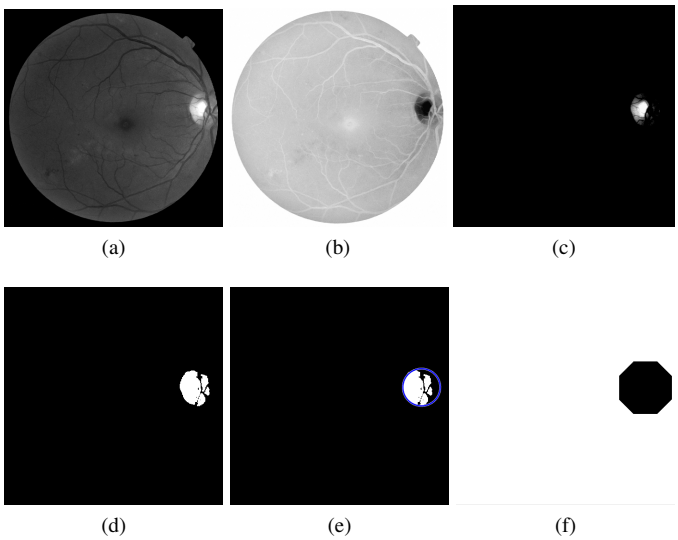

Fig. 4. Optical disc detection: (a) Equalized green component, (b) Equalized cyan component, (c) Difference between *a* and *b* images, (d) Binarized and dilated image, (e) Hough transform: blue circumference is its result, (f) Optical-disc mask.

4) Summary of features: In summary, the 8 quantitative features used by our classifier are:

1) Standard deviation of the red component.
2) Standard deviation of the green component.
3) Standard deviation of the blue component.
4) Blood vessel density.
5) Possible number of microaneurysms.
6) Actual number of microaneurysms.
7) Density of hard exudates.
8) Green component entropy.

III. Results

The evaluation of our proposal was implemented in the software Matlab® and has been split in two subsections: NPDR detection and NPDR grade classification.

A. NPDR Detection

The main idea of this first set of results is to detect any grade of NPDR. For that, we used 301 retinal images, 152 with grade 0 and 149 with grade 3. We trained a SVM classifier with all the features of these images and then tested it through a 10-fold cross-validation process. The performance was also optimized selecting the most relevant features and SVM parameters.

Thus, the best accuracy of our detector was obtained using a linear kernel function in the SVM algorithm. In this case, SVM only requires the possible number of microaneurysms and the actual number of microaneurysms as input features. The confusion matrix of the best detector is shown in Table I. In order to contrast our SVM results, we have also implemented a decision-tree (DT) classifier based on the Gini-index. The best performance for the DT was obtained when the actual number of microaneurysms is the only used input. Table II summarizes the accuracy, sensibility, specificity and area under the ROC curve (AUC) results. Note that the AUC value estimates the predictive capacity of the classifier.

Since this kind of applications normally requires optimizing sensibility rather than accuracy, Table III shows results under this new constraint. The best sensibility was obtained with SVM and a Gaussian kernel function with gamma equals to 0.71. On the other hand, DT showed the best sensibility with a depth of 9. These last SVM and DT detectors require all 8 extracted features to improve their sensibility.

B. NPDR Grade Classification

Besides the detection of NPDR, we are also interested in classifying the NPDR grade. For that, we used all the 400 retinal images. A multi-class SVM (one-to-one) classifier was trained with all the features and then tested using a 10-fold cross validation. The final performance was optimized selecting the most relevant features and SVM parameters.

TABLE I
CONFUSION MATRIX FOR THE ACCURACY-OPTIMIZED NPDR DETECTOR.

$n = 301$	Predicted NO	Predicted YES
Actual NO	148	4
Actual YES	19	130

TABLE II
ACCURACY-OPTIMIZED PERFORMANCE OF SVM AND DT DETECTORS.

Metric	SVM	Decision-tree
Accuracy	**92.4**%	92.0%
Sensibility	87.3%	86.6%
Specificity	97.4%	97.4%
AUC	93.8%	88.7%

TABLE III
SENSIBILITY-OPTIMIZED PERFORMANCE OF SVM AND DT DETECTORS.

Metric	SVM	Decision-tree
Accuracy	80.4%	91.0%
Sensibility	**94.6**%	94.0%
Specificity	66.2%	88.1%
AUC	89.9%	90.8%

TABLE IV
CONFUSION MATRIX FOR THE ACCURACY-OPTIMIZED CLASSIFIER.

$n = 400$	Grade 0	Grade 1	Grade 2	Grade 3
Grade 0	148	0	1	3
Grade 1	25	0	2	3
Grade 2	29	0	14	26
Grade 3	20	0	10	119

When the accuracy of the classifier was the main metric to optimize, we obtained the confusion matrix showed in Table IV. The best performance was acquired using a multi-class SVM with a lineal kernel function. The selected features in this case were the actual number of microaneurysms, blood vessel density and standard deviation of the blue component. Table V summarizes accuracy, sensibility, specificity and AUC results. In the case of the DT classifier, it was necessary to set its maximum depth to 4 and to include 5 features: possible number of microaneurysms, actual number of microaneurysms, density of hard exudates, standard deviations of the red and green components. Table VI shows a summary of these last results.

IV. DISCUSSION

Our results show that NPDR detection reaches an accuracy of 92.4%, although the sensibility is reduces by the presentce of 19 false negatives (Table I). A big challenge here is the non-detection of microaneurysms in some retinal images. However, when the aim is to optimize sensibility, the number of false negatives is reduced to 8 and the sensibility reaches 94.6%.

In the case of NPDR grade classification the situation is a little bit different. The asymmetry in the number of samples for each class (*e.g.*, 152 grade-0 samples, 30 grade-1 samples) reduces the accuracy of the classifier. However, we can see that the sensibility for NPDR grade 0 (*i.e.*, no NPDR) can reach 97%, while the accuracy for mild NPDR (*i.e.*, grade 1) is 92.5%. The average accuracy of the classifier reaches 85%.

All results from the SVM detector and classifier are consistently better than the corresponding DT results. SVM results are also similar to those published in previous works [2]. This proves the robustness of our proposed SVM implementation.

TABLE V
PERFORMANCE OF THE SVM CLASSIFIER.

Metric	Grade 0	Grade 1	Grade 2	Grade 3	Average
Accuracy	80.5%	92.5%	83.0%	84.5%	85.1%
Sensibility	97.4%	0.0%	20.3%	79.9%	49.4%
Specificity	70.2%	100.0%	96.1%	87.3%	88.4%
AUC	83.9%	62.6%	70.9%	90.7%	77.0%

TABLE VI
PERFORMANCE OF THE DECISION-TREE CLASSIFIER.

Metric	Grade 0	Grade 1	Grade 2	Grade 3	Average
Accuracy	80.5%	92.5%	82.3%	85.3%	85.1%
Sensibility	96.7%	0.0%	18.8%	81.2%	49.2%
Specificity	70.6%	100.0%	95.5%	87.6%	88.4%
AUC	83.5%	62.6%	70.4%	92.7%	77.3%

V. CONCLUSIONS

Efficient algorithms for the detection of blood vessels, microaneurysms, the optic-disc, and hard exudates have been presented. The proposed features show a great potential for NPDR detection and classification. SVM can detect NPDR with a sensibility of almost 95%, while NPDR can be classified with an average accuracy of 85%. SVM consistently shows better results that other machine learning algorithms. We can conclude that image processing of retinal images has the potential to play a major role in diagnosis of diabetic retinopathy. The results are encouraging and a future clinical evaluation will integrate the presented algorithms in a tool for diagnosis of diabetic retinopathy. Other future works are the detection of soft exudates, besides hard exudates, and the application of texture analysis in order to improve accuracy and sensibility of our retinopathy detector.

ACKNOWLEDGMENT

This work was supported by a research grant from Universidad de las Fuerzas Armadas ESPE (2015-PIC-004).

REFERENCES

[1] B. Wu, W. Zhu, F. Shi, S. Zhu, and X. Chen, "Automatic detection of microaneurysms in retinal fundus images," *Computerized Medical Imaging and Graphics*, vol. 55, pp. 106–112, 2017.

[2] R. Maher, S. Kayte, and D. M. Dhopeshwarkar, "Review of automated detection for diabetes retinopathy using fundus images," *International Journal of Advanced Research in Computer Science and Software Engineering*, vol. 5, no. 3, pp. 1129–1136, 2015.

[3] D. J. Browning, *Diabetic retinopathy: evidence-based management*. Springer Science & Business Media, 2010.

[4] R. Maher, S. Kayte, D. Panchal, P. Sathe, and S. Meldhe, "A decision support system for automatic screening of non-proliferative diabetic retinopathy," *International Journal of Emerging Research in Management and Technology*, vol. 4, no. 10, pp. 18–24, 2015.

[5] R. S. Maher, S. N. Kayte, S. T. Meldhe, and M. Dhopeshwarkar, "Automated diagnosis non-proliferative diabetic retinopathy in fundus images using support vector machine," *International Journal of Computer Applications*, vol. 125, no. 15, pp. 7–10, 2015.

[6] B. Singh and K. Jayasree, "Implementation of diabetic retinopathy detection system for enhance digital fundus images," *International Journal of advanced technology and innovation research*, vol. 7, no. 6, pp. 874–876, 2015.

[7] N. Thomas and T. Mahesh, "Detecting clinical features of diabetic retinopathy using image processing," *International Journal of Engineering Research & Technology (IJERT)*, vol. 3, no. 8, pp. 558–561, 2014.

[8] M. Gandhi and R. Dhanasekaran, "Diagnosis of diabetic retinopathy using morphological process and SVM classifier," in *Communications and Signal Processing (ICCSP), 2013 International Conference on*. IEEE, 2013, pp. 873–877.

[9] E. M. Shahin, T. E. Taha, W. Al-Nuaimy, S. El Rabaie, O. F. Zahran, and F. E. A. El-Samie, "Automated detection of diabetic retinopathy in blurred digital fundus images," in *Computer Engineering Conference (ICENCO), 2012 8th International*. IEEE, 2012, pp. 20–25.

[10] E. Decencière, X. Zhang, G. Cazuguel, B. Lay, B. Cochener, C. Trone, P. Gain, R. Ordonez, P. Massin, A. Erginay, B. Charton, and J.-C. Klein, "Feedback on a publicly distributed database: the Messidor database," *Image Analysis & Stereology*, vol. 33, no. 3, pp. 231–234, Aug. 2014.